

## NANO CRYSTALLINE ZnO THIN FILMS REINFORCED WITH MWCNT BASED BUCKYPAPERS AS NEGATIVE ELECTRODES FOR LITHIUM ION BATTERIES

M.O. Guler<sup>1\*</sup>, O. Cevher<sup>1</sup>, U. Tocoglu<sup>1</sup>, H. Akbulut<sup>1</sup>

<sup>1</sup>Sakarya University, Engineering Faculty, Metallurgical & Materials Engineering Department, Esentepe Campus, 54187, Sakarya, Turkey

\*guler@sakarya.edu.tr

**Keywords:** Li-ion batteries, zinc oxide, multiwall carbon nanotubes, anode.

### Abstract

*In this study, magnetron sputtering technique for synthesis of ZnO–CNT nanocomposites, which consist of highly dispersed 2.90–7.47 nm ZnO nanocrystals on the surface of buckypapers produced via simple vacuum infiltration techniques by using multiwalled carbon nanotubes (CNTs). As anode materials for Li-ion batteries, the nanocomposites showed high rate capability and superior cycling stability with specific capacity of 760 mAh g<sup>-1</sup> for up to 100 cycles. The CNTs served as electron conductors and volume buffers in the nanocomposites.*

### 1 Introduction

Semiconductor metal oxides are well known potential alternative to carbonaceous materials as anode materials of commercial lithium ion batteries and they have higher reversible capacities even at high current densities. The most popular oxides are tin and tin-based composite oxide and alloys, transition metal oxides such as iron, cobalt, nickel and copper oxides and zinc oxide. Among the above oxides, zinc oxide has so many advantages such as easy to prepare, low cost and chemically stable [1-4]. As an anode material in lithium ion batteries, ZnO has a theoretical capacity of 978 mAh g<sup>-1</sup> while carbonaceous anode materials have 372 mAh g<sup>-1</sup> [5-7]. However, it is rarely investigated in the lithium ion batteries due to the severe capacity fade upon cycling even at low densities and may drop down to 200 mAh g<sup>-1</sup> after a few cycles. The main reason is that the ZnO material has low electrical conductivity and the electrodes made of ZnO material often suffers the loss of electrical contact with the current collector due to high volumetric expansion during intercalation process with lithium ions (volumetric expansion is up to > 300%) [8,9]. To overcome this problem, many researchers are focusing on synthesis of metal oxide nanoparticles, which are able to better accommodate the mechanical stress experienced during volume changes [10]. Another approach is the use of carbon as matrix support on which metal oxide nanoparticles are attached [11]. Among various kinds of carbon materials, the carbon nanotube is attractive due to its high electrical conductivity, high aspect ratio, remarkable thermal conductivity, and good mechanical properties, which can improve the electrode's reversible capacity and rate capability [12]. Using CNTs as reinforcing elements as in the form of buckypapers seems to be a good solution for lithium ion batteries. A recent approach to involves initially forming macroscopic free standing porous sheets or entangled nanotubes called buckypapers and then

manufacturing the buckypaper composite through infiltrating metal oxides into the buckypaper pores made of multiwall carbon nanotubes (MWCNTs).

In this study, carbon nanotube thin sheets – buckypapers – were prepared from multi-walled carbon nanotubes oxidised with different oxidation agents. Buckypapers were then coated with magnetron sputtering route for the synthesis of ZnO–CNT nanocomposites, which consist of highly dispersed ZnO nanocrystals with diameters of 2.90–7.47 nm that are deposited on the outer surface of CNTs. The surface morphology, phase composition and electrochemical efficiencies were studied in detail.

## 2 Experimental Details

### 2.1 Electrode fabrication procedures

The MWCNT employed in this work was supplied by Arry International (Germany). The nanotubes were synthesized by catalytic carbon vapour deposition (CCVD) and had a purity of around 80%. The CNT diameter ranged between 10 and 20 nm. Purification and chemical oxidation of MWCNTs was carried out with different oxidation agents supplied by Aldrich. 1 g of the as-received MWCNTs were dispersed in 25 ml of the nitric acid (65 wt%) in a 100 ml round bottom flask equipped with a condenser and the dispersion was refluxed under magnetic stirring for 48 h. After that, the resulting dispersion was diluted in water and filtered. The resulting solid was washed up to neutral pH, and the sample was dried in vacuum at 40 °C overnight. Concerning the fabrication of MWCNT buckypapers, stable aqueous CNT suspensions at a concentration of 1mg/ml were prepared by tip sonication for 60 min. These dispersions were then vacuum filtered through polycarbonate membrane filters of 450 nm pore size. After drying at room temperature in a vacuum oven for 24 h the CNT films were peeled off from the filtration membrane. The average thickness of the produced buckypapers is approximately 200 µm and their diameter about 16 mm.

ZnO thin films were deposited by RF magnetron sputtering using a sintered ZnO target (2 inch, 99.99%, Kurt Lesker Company). The sputtering chamber was evacuated to  $4 \times 10^{-4}$  Pa using a turbomolecular pump prior to the introduction of the Ar–O<sub>2</sub> gas mixture. The total working pressure, the oxygen content and the RF input power was, 0.55 Pa, 0–10% and the 100 W, respectively. The distance between the ZnO target and the buckypaper substrate and the substrate temperature were maintained at 13 cm and 25 °C, respectively.

### 2.2 Characterization

The phase structures of the deposited films were investigated by X-ray diffraction (XRD) (Rigaku D/MAX 2000 with thin film attachment) with Cu K<sub>α</sub> radiation. The grain size of the thin films was calculated from the Scherrer's formula [13];

$$D = \frac{0.9\lambda}{B \cos \theta} \quad (1)$$

where D is the mean grain size,  $\lambda$  is the X-ray wavelength, B is the corrected full-width at half maximum (FWHM) and  $\theta$  is the Bragg angle.

The morphology was observed by scanning electron microscopy (JSM-6060 LV system). Coin-type (CR2016) test cells were assembled in an argon-filled glove box, directly using the

ZnO coated CNT buckypapers as the working electrode, a lithium metal foil as the counter electrode, a micro porous polypropylene (PP) membrane (Cellgard 2400) as the separator, and 1M solution of LiPF<sub>6</sub> in ethylene carbonate (EC) and dimethyl carbonate (DMC) (1:1 by weight) as the electrolyte. The cells were aged for 12h before measurements. The cells were cyclically tested on a MTI Model BST8-MA electrochemical analyzer using different current densities over a voltage range of 1–3V.

### 3. Results and Discussion

#### 3.1 XRD analysis

XRD patterns for the as-produced buckypaper and ZnO thin films deposited under various oxygen partial pressures are depicted in Fig. 1. All reflexes were assigned to Carbon (JCPDS 026-1080) and hexagonal zinc oxide (JCPDS-36-1451). As the oxygen partial pressure increases to 10%, the intensity of ZnO (002) peak increases remarkably and the (103) peak disappears. Higher oxygen partial pressure provides more energy to enhance mobility of the deposition atoms, which improves the crystal quality of the films. As the oxygen partial pressure further increases, the films exhibit only (002) peak, indicating that the films are highly oriented with c-axis perpendicular to the substrates.

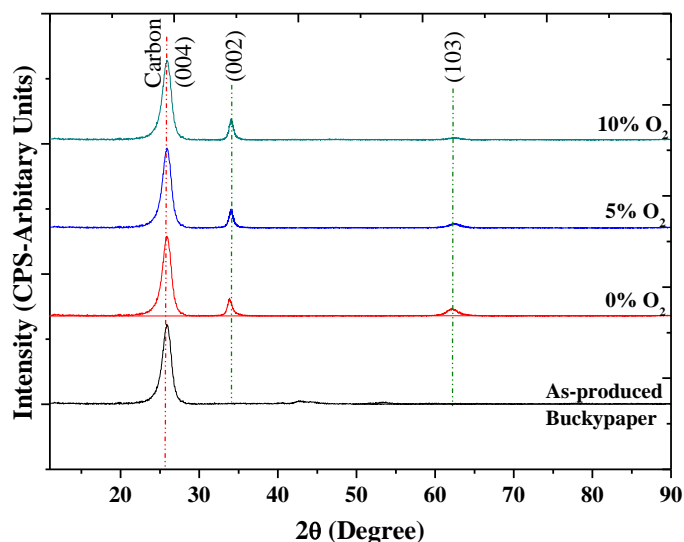


**Figure 1.** XRD patterns of produced MWCNT based buckypaper and ZnO coatings at various oxygen partial pressures.

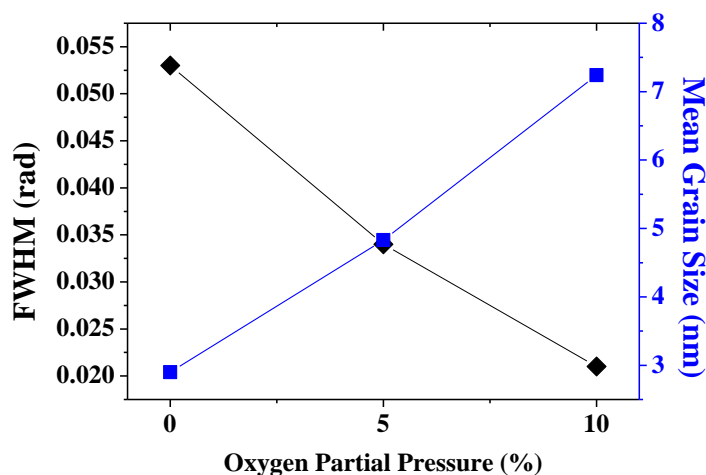


**Figure 2.** FWHM and crystal size for the ZnO thin films as a function of oxygen partial pressure.

## 3.2 SEM analysis

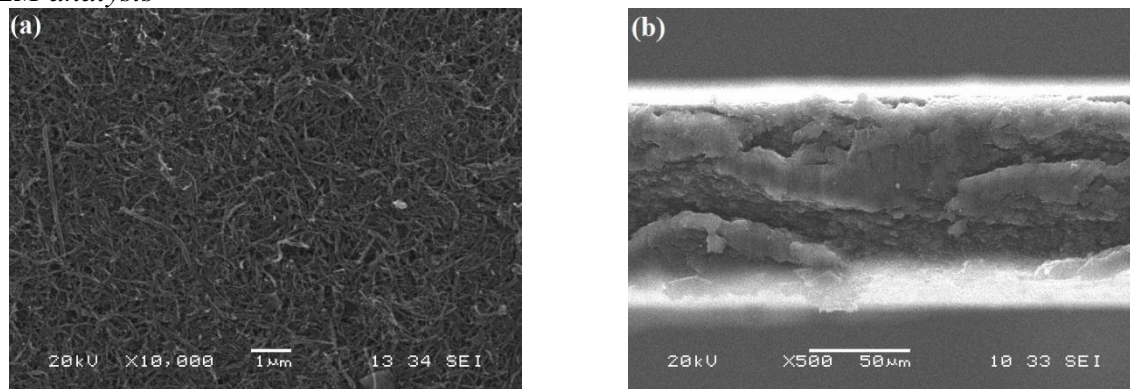


**Figure 3.** Typical SEM images of (a) surface and (b) cross-section area of the as-produced buckypaper.

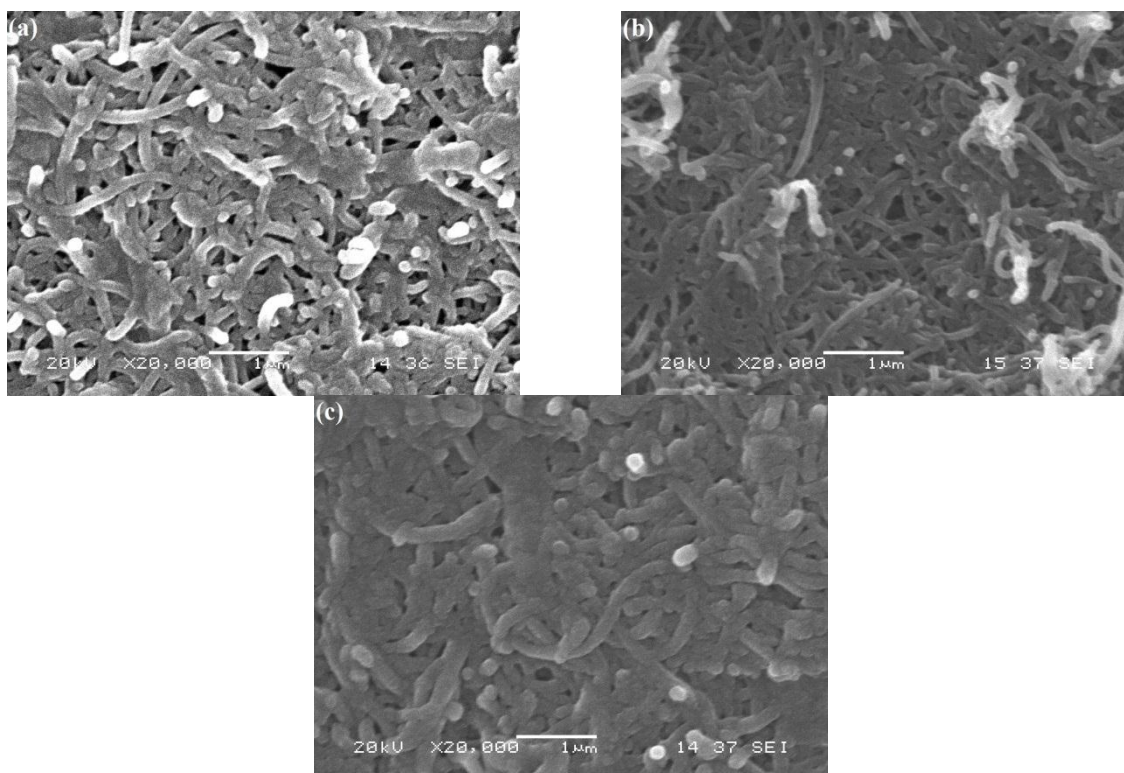


**Figure 4.** SEM images of the films deposited under (a) 0%, (b) 5% and (c) 10% oxygen partial pressures.

Buckypapers prepared by vacuum filtration of well-dispersed CNT aqueous suspensions were found to be uniform, smooth and crack-free disks exhibiting significant structural integrity, as confirmed by SEM images (Fig. 3). The produced thin films consist of randomly interconnected CNTs forming a porous structure as it is apparent from Fig. 3a. The SEM image of a cross-section of a representative sheet (Fig. 3b) indicates an almost homogeneous CNT deposition through the thickness giving rise to a dense morphology. For comparison, Fig. 4 shows an SEM image of the ZnO–CNT nanocomposite, in which ZnO is considered to be selectively nucleated and uniformly deposited on the surface of CNTs by the magnetron sputtering process. No obvious separated ZnO bulk particles are evident apart from those deposited on CNTs. The CNTs coated with ZnO are entangled and interconnected to form a uniform network with a three-dimensional structure.

### 3.3 Electrochemical analysis

The discharge–charge profiles of ZnO thin films are illustrated in Fig. 5. The CNT:ZnO nano composite electrode delivers an initial discharge capacity of  $1461 \text{ mAh g}^{-1}$ , while 100<sup>th</sup> cycle discharge capacity is close to  $760 \text{ mAh g}^{-1}$  for the films deposited under 0% oxygen partial pressure. It is interesting to find that the ZnO:CNT nano composites exhibit much higher lithium storage capability than the bulk ZnO. Such enhancement of capacity is due to the large surface area and short diffusion distance offered by the nanorod arrays. It is reasonable that the large surface area of the ZnO:CNT nano composites provide sufficient space for lithium storage, including lithium–zinc alloy formation, the growth of the organic-like-layer [14] as well as interfacial interaction toward lithium [15].

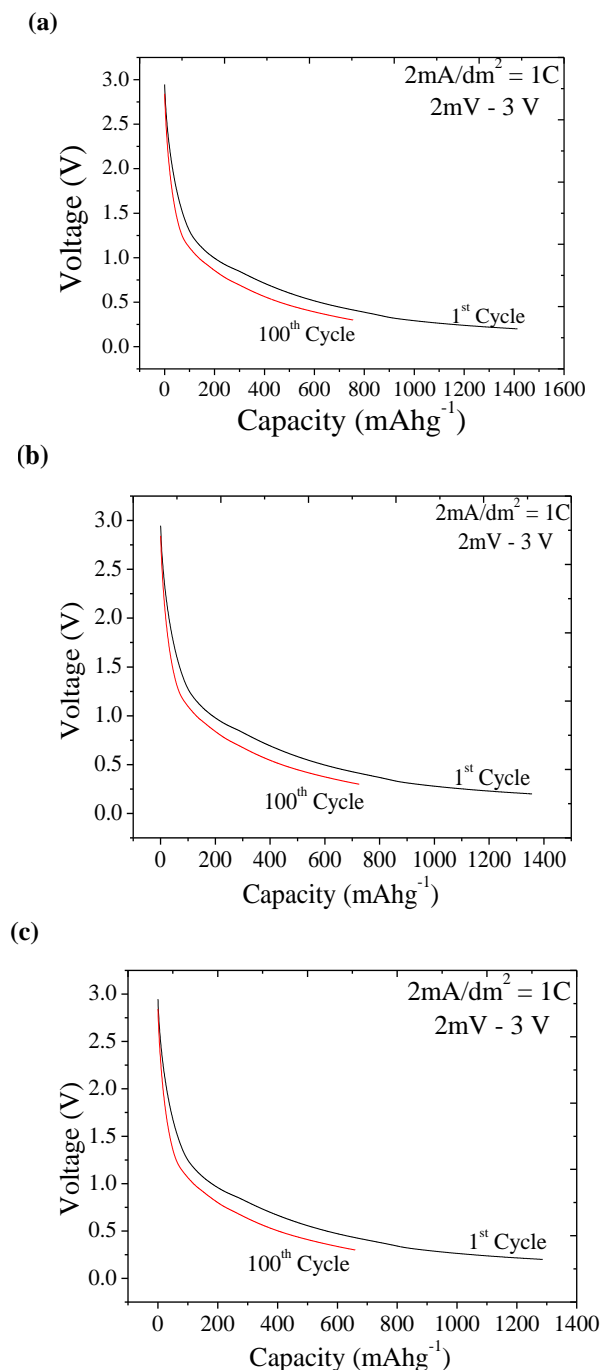


**Figure 5.** Voltage - Discharge Capacity graphics of the films deposited under (a) 0% Oxygen, (b) 5% Oxygen and (c) 10% Oxygen partial pressures.

All of the fresh-prepared cells made from ZnO:CNT nano composites were cycled at the current density of  $0.2 \text{ mAcm}^{-2}$  to investigate their cyclabilities, and the results are shown in Fig. 6. Compared with the films deposited under various oxygen partial pressures, the cells deliver low discharge and charge capacities at this higher current density. It can be seen that the capacities drop slowly in the first 80 cycles, and then maintain at about  $760 \text{ mAhg}^{-1}$ ,  $723 \text{ mAhg}^{-1}$  and  $654 \text{ mAhg}^{-1}$  up to 100 cycles with no significant fading for the films deposited under 0%, 5% and 10% oxygen partial pressures, respectively. Obviously, the cycling performance of the ZnO:CNT nano composites are much better than the commercial ZnO powders. It is reported that many unmodified ZnO material's capacities often drop very quickly upon cycling even at low current densities [16].

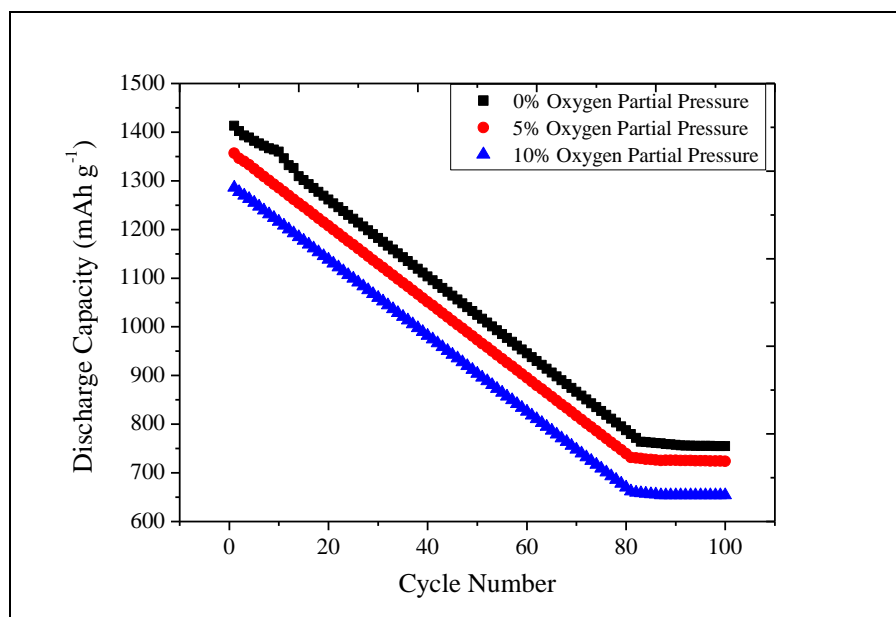


**Figure 5.** Voltage - Discharge Capacity graphics of the films deposited under (a) 0% Oxygen, (b) 5% Oxygen and (c) 10% Oxygen partial pressures.

#### 4. Conclusions

In summary, a ZnO–CNT nanocomposite was successfully synthesized by magnetron sputtering techniques onto as-produced MWCNT based freestanding electrodes also known as buckypapers. The highly dispersed ZnO nanocrystals with crystal size of 2.90–7.47 nm were uniformly deposited onto the surface of CNT based buckypapers. As anode material for Li-ion battery, the nanocomposites presented a superior cycling stability up to 100 cycles with a capacity of  $760 \text{ mAh g}^{-1}$ . Such good stability was ascribed to the strong adhesion of ZnO nanocrystals on the CNT support, which has high electronic conductivity and possesses good flexibility. The strategy presented in this paper could be extended to the synthesis of other metal oxide (e.g.,  $\text{MnO}_x$ ,  $\text{FeO}_x$ ,  $\text{CoO}_x$ ,  $\text{TiO}_2$ , and  $\text{SnO}_2$ ) composites with different carbon materials.

#### References

- [1] Poizot P., Laruelle S., Grugeon S., Dupont L., Tarascon J.M. Nano-sized transition-metal oxides as negative-electrode materials for lithium-ion batteries. *Nature*, **407**, 496-499 (2000).

- [2] Taberna L., Mitra S., Poizot P., Simon P., Tarascon J.M. High rate capabilities Fe<sub>3</sub>O<sub>4</sub>-based Cu nano-architected electrodes for lithium-ion battery applications. *Nat. Mater.*, **5** 567-573 (2006).
- [3] Liu B., Zeng H.C. Mesoscale organization of CuO nanoribbons: formation of "Dandelions". *J. Am. Chem. Soc.*, **126**, 8124-8125 (2004).
- [4] Li H., Balaya P., Maier J. Li-storage via heterogeneous reaction in selected binary metal fluorides and oxides. *J. Electrochem. Soc.*, **151**, A1878-A1885 (2004).
- [5] Yu Y., Chen C.H., Shi Y. A tin-based amorphous oxide composite with a porous, spherical, multideck-cage morphology as a highly reversible anode material for lithium-ion batteries. *Adv. Mater.*, **19**, 993-997 (2007).
- [6] Jamnik J., Maier J. Nanocrystallinity effects in lithium battery materials: Aspects of nano-ionics. Part IV. *Phys. Chem. Chem. Phys.*, **5**, 5215-5220 (2003).
- [7] Belliard F., Connor P.A., Irvine J.T.S. Doped tin oxides as potential lithium ion battery negative electrodes. *Ionics*, **5**, 450-454 (1999).
- [8] Belliard F., Connor P.A., Irvine J.T.S. Novel tin oxide-based anodes for Li-ion batteries. *Solid State Ionics*, **135**, 163-167 (2000).
- [9] Li H., Huang X., Chen L. Anodes based on oxide materials for lithium rechargeable batteries. *Solid State Ionics*, **123**, 189-197 (1999).
- [10] Ng S.H., Santos D.I., Chew S.Y., Wexler D., Wang J., Dou S.X., Liu H.K. Polyol-mediated synthesis of ultrafine tin oxide nanoparticles for reversible Li-ion storage. *Electrochem. Commun.*, **9**, 915-919 (2007).
- [11] Zhang H.X., Feng C., Zhai Y.C., Jiang K.L., Li Q.Q., Fan S.S. Cross-stacked carbon nanotube sheets uniformly loaded with SnO<sub>2</sub> nanoparticles: a novel binder-free and high-capacity anode material for lithium-ion batteries. *Adv. Mater.*, **21**, 2299-2304 (2009).
- [12] Wen Z., Wang Q., Zhang Q., Li J. In situ growth of mesoporous SnO<sub>2</sub> on multiwalled carbon nanotubes: a novel composite with porous-tube structure as anode for lithium batteries. *Adv. Funct. Mater.*, **17**, 2772-2778 (2007).
- [13] Chan y Diaz E., Juan M. C., Moller A. D., Rodrigues R. C., Perez P. B., Influence of the oxygen pressure on the physical properties of the pulsed-laser deposited Te doped SnO<sub>2</sub> thin films. *J. Alloys and Compound*. **508**, 342-347 (2010).
- [14] Laruelle S., Grugeon S., Poizot P., Dolle M., Dupont L., Tarascon J.M. On the origin of the extra electrochemical capacity displayed by MO/Li cells at low potential *J. Electrochem. Soc.*, **149**, A627-A634 (2002).
- [15] Li H., Richter G., Maier J., Reversible formation and decomposition of lif clusters using transition metal fluorides as precursors and their application in rechargeable li batteries. *Adv. Mater.* **15**, 736-739 (2003).
- [16] Zhang C.Q., Tu J.P., Yuan Y.F., Huang X.H., Chen X.T., Mao F. Electrochemical performances of Ni-coated ZnO as an anode material for lithium-ion batteries *J. Electrochem. Soc.* **154** A65-A69 (2007).